Acta Oceanol. Sin., 2023, Vol. 42, No. 9, P. 44–52
https://doi.org/10.1007/s13131-023-2154-1
http://www.aosocean.com
E-mail: ocean2@hyxb.org.cn

Morphometric analysis of the Andaman outer shelf and upper slope—Implications for the recent slope failure events

Pachoenchoke Jintasaeranee[1]*, Anond Snidvongs[2]

[1] Department of Aquatic Science, Faculty of Science, Burapha University, Chonburi 20131, Thailand

[2] Department of Marine Science, Faculty of Science, Chulalongkorn University, Bangkok 10330, Thailand

Received 5 December 2021; accepted 28 October 2022

Abstract

The devastating 2004 tsunamis that hit the southwestern coast of Thailand pose a serious threat to people along the coastal zone. A major aim for the tsunami hazard prediction is better prediction of the next tsunamis and their impacts. In this paper, we present the first implications of recent slope failure events of the Andaman outer shelf and upper slope based on a new detailed bathymetric data and subbottom profiler records acquired during two cruises of the MASS project in 2006 and 2007. Morphometric analysis reveals a variety of anomalous features, including: three large plateaus surrounded by moats, ruggedness and unevenness of slope morphology, and two translational submarine landslides. Two submarine landslides are studied from the detailed bathymetric data and subbottom profiler record covering the upper slope of the Andaman Sea shelf break within Thai exclusive economic zone. Maximum approximated volumes of both displaced masses are 4.8×10^7 m^3 and 2.2×10^7 m^3. Considering the data, there is no evidence that landslides have been the sources for tsunami hazard potential in recent geological time. These prerequisites will allow better study of slope failure events in the area. Further investigation is required to better understand obvious geotectonic phenomena.

Key words: Andaman, slope failure, submarine landslide, bathymetry, hazard potential

Citation: Jintasaeranee Pachoenchoke, Snidvongs Anond. 2023. Morphometric analysis of the Andaman outer shelf and upper slope—Implications for the recent slope failure events. Acta Oceanologica Sinica, 42(9): 44–52, doi: 10.1007/s13131-023-2154-1

1 Introduction

Mass failures are common occurrences along slopes of various continental margins. The occurrences are generally associated with sediment mobility (Jenkins and Keene, 1992; Sultan et al., 2004, 2007; von Huene et al., 2004; Jackson et al., 2004; Vanneste et al., 2006; Locat et al., 2009; Loncke et al., 2009a, b). Through the inducement of gravity, movements of the sediment generally lead to failures of slopes (Mulder and Cochonat, 1996; Masson et al., 2002; Silva et al., 2004; Seeber et al., 2007; Levchenko et al., 2008; Locat et al., 2009; Bellec et al., 2010). The failure events may involve a variety of sediment mobilities ranging from sediment creep to submarine landslide (Mulder and Cochonat, 1996; Moscardelli et al., 2006; Bull et al., 2009; Sun et al., 2018).

Increasing economic activities along coastal areas have increased the need for better understanding submarine slope failures events that are a potential significant cause of natural hazards to the coastlines (Terry et al., 2017; Sun and Leslie, 2020; Pan et al., 2022). Unfortunately, direct observation and measurement of the processes are generally impossible due to the irregular nature of the failure events. However, morphometric analysis makes indirect observation of submarine slope failures possible. The analysis involves characterization of near-surface seafloor sediment movements which can be mostly distinguished by a high resolution bathymetric chart (Hampton et al., 1996; Mulder and Cochonat, 1996; Brune et al., 2010a, b, c) and related to the corresponding subbottom profiler records (Damuth and Hayes, 1977; Damuth, 1975, 1978, 1980; Pratson and Laine, 1989; Chough et al., 1997; Reddy and Rao, 1997; Lee and Baraza, 1999; Lee et al., 2002; Mosher et al., 2008).

On the outer shelf of the southwestern of Mergui Ridge in the Andaman Sea within the Thai exclusive economic zone (EEZ), generally no hydroacoustic data have been available for geotectonic study before the 2004 tsunamis. Recently, an area of about 3 000 km^2 covering the upper slope of the outer shelf was investigated using subsurface hydroacoustic surveys under the framework of the project "Morphodynamics and Slope Stability of the Andaman Sea Shelf Break" (MASS). In this paper, we determine the morphology of the western slope of Mergui Ridge and identify scarps, headwalls, escarpments, debris toes and other manifestations of slope failures and downslope mass transport, and current state of the slope area derived from high resolution bathymetry and present the recent submarine slope failure features and morphodynamic submarine landslides. These prerequisites are needed for a better understanding of the current status of the slope and supporting better information for tsunami hazard assessments in the Andaman Sea.

2 Geological setting, sedimentology and oceanography

An area on the seafloor of the East Andaman Sea is characterized as an active backarc basin between the Andaman-Nicobar-Islands, Sumatera and the west coast of the Peninsular Malaysia (Curray, 2005). From a tectonic point of view, the east basin could be related to several stages of reconstruction and formation faults. Various strike-slip faults generally lying on a N–S direction are currently considered as the active faults zone, however, their positions are current poorly known (Polachan and

Foundation item: The Financial Support Jointly by the National Research Council of Thailand and the German Research Foundation.
*Corresponding author, E-mail: pachoenc@go.buu.ac.th

Racey, 1993; Curray, 2005; Tingay et al., 2010). In addition, a pull-apart extension of the fault in the central basin could affect the east basin. The fault is generally oriented on NE–SW direction and probably started approximately 4 Ma ago with initial rate of about 1.6 cm/a and about 3.8 cm/a at present (Raju et al., 2004; Khan and Chakraborty, 2005). Moving of the extensional fault could make the east basin compress and also could possibly generate pathways for fluid escape from shallow sub-seafloor, especially the Mergui Ridge.

The surface of the Mergui Terrace is covered largely by muddy sand and small shell-fragments. These compositions render the sediment poorly sorted. The Irrawaddy Rivers discharge could be a source of sediments supply to the terrace (Rodolfo, 1969) at a rate of over 360×10^6 t (Rao et al., 2005). Approximately 70% of the sediment settles at the rivers delta, while the rest could be delivered through Mataban Canyon to the deeper part and accumulated on the seafloor far from the source (Ramaswamy et al., 2004). The sediment transportation through the deeper areas might be accomplished by some types of gravity-controlled sediment phenomena, and forms the basin (Rodolfo, 1969; Rao et al., 2005). The graded beds are up to few meters thick and comprise surface-layer sediment and associated structures of the shelf. It is suggested that the sediment deposition was primarily by turbidity currents with a sedimentation rate below 10 mm/1 000 a (Rodolfo, 1969). A pelagic component of interbedded sediment such as foraminiferal ooze suggests that these sediments accumulated continuously and slowly (Saidova, 2008).

On Mergui Basin, sediments have been studied by three wells drilling. The upper thin layer of sediment on the seafloor of about 180–240 m thickness comprises silty shales and fine-grained sandstones, whereas the lower layer of sediment of about 700–1 000 m thickness comprises coral/algal limestones. The sediment in between both layers reveals a thin layer of sediment turbidites (Polachan and Racey, 1993). In addition, the sediment core of the Sumatera shelf basin reveals a very thin volcanic clayey sand layer below the core top (Rodolfo, 1969). This interpretation may draw sediment processes on the area which could be the turbidity current deposit. The interpretation also suggests another source of terrigenous sediments which could supply the basin from the Sumatera–Malacca stream southward.

As the Andaman Sea locates under the effects of the Southeast Asia monsoon systems, generally, winds of the SW monsoon (summer winds) blow steadily at a rate more than twice of the NE monsoon (winter winds). Arrival of strong summer winds dramatically drive the westerly current towards the prevailing southeasterly current, resulting in the transportation of riverine sediment moving eastward along the inner shelf (Rodolfo, 1969; Ramaswamy et al., 2004; Rao et al., 2005). In contrast, the winter winds cause south-easterly currents to flow towards westerly currents. The north-westward current in the Malacca strait is generally restricted to the northern part of Sumatera. The sediments are forced and transported by Sumatera streams from the strait into the south Andaman Sea throughout the year as the density flows (Rodolfo, 1969).

Little is known about the seafloor and the tectonic structure of the Thai EEZ of the Andaman Sea. According to global bathymetric data GEBCO 1-min (IOC et al., 2003), the western rim of the Mergui Ridge forms an escarpment-like structure with steep slopes up to a maximum value of about 4.5° may originate submarine landslides on the surface slope (Hampton et al., 1996) and their significant potential tsunamis. Major causes of the landslides are the characters of the sediment and its properties. Especially, fine-grained sediment deposits with high water content can be extremely under consolidated and lead to slope failure events. Another cause is slope steepness. Increasing of slope angle might lead to over steepening and eventually slope failures (Mulder and Cochonat, 1996; Hampton et al., 1996; Leynaud et al., 2009; Brune et al., 2010c; Sun et al., 2018). Nevertheless, the resolution of these datasets is very coarse and only based on satellite information or very sparse single beam soundings. Therefore, locally there well may exist much steeper slopes. To date no high-resolution bathymetric data by a high-resolution multibeam bathymetric survey from the Mergui Ridge is available for research and scientific communities and is critical in need to image the morphology of Mergui Ridge and slope.

3 Data collection and processing

The surveys on the upper slope of the Andaman Sea shelf break within Thai EEZ (Fig. 1) were conducted on board of Thai R/V Chakratong Tongyai of the Department of Marine and Coastal Resources, Ministry of Natural Resources and Environment, Thailand during two cruises in November–December 2006 and October–November 2007. The survey cruises covered the southwestern corner of the Thai EEZ, which forms the southern end of the Mergui Ridge by a topographic rise that stretches through the central Andaman Sea in north–south direction. Water depths in the survey area varied from about 500 m on the top of the Mergui Ridge to more than 1 400 m at the southwestern edge of the area. The bathymetric data was collected using the Seabeam 1050 Multibeam Echosounder and the parametric data were collected using the INNOMAR SES 2000 medium Subbottom Profiler. During the surveys, some transducer arrays were damaged resulting in some continuous bathymetric data being unavailable near the southern part of the investigated area. In addition, the vibration of the pole limited the range of the bathymetric data to generally less than 1 500 m water depth. The penetration of the parametric signals into the sub-seafloor was generally less than 10 m with maximum values of 15 m. The bathymetric grid was processed by using the MB-System (Caress and Chayes, 2004) and displayed by using the Generic Mapping Tool-GMT (Wessel and Smith, 1998). The subbottom profiler records were processed using the traditional SES software and subsequently imported into the KINGDOM suite in order to analyze echo-characters. The multibeam echosounding data have been processed by various visualization techniques to image for the morphology of the area in great detail to determine possible submarine landslide features. The theoretical tsunami wave length and maximum amplitude directly over the slope failure generated by disintegrative submarine landslides can be calculated by the semi empirical equations proposed by Watts et al. (2003) and McAdoo and Watts (2004).

4 Results

When using the depth accuracy tests, it revealed that 95% of the processed grids obtained values equal or better than 1% of water depth. This is acceptable for the generation of a final grid (Beyer et al., 2003, 2005; de Alteriis et al., 2003) when grid resolution has been set to 50 m (Fig. 2). The depth accuracy of the instrument can be linked to the standard deviation, thus the values should vary between 5 m and 16 m height. This test also reveals that 95% of the grid cells obtained standard deviations better than 16 m height. The new detailed bathymetric data and subbottom profiler record covering the upper slope of the Andaman Sea shelf break within Thai EEZ of approximately 3 000 km^2 allows the characterization of general morphology of the slope and eventually reveals previously unknown anomalous features on the seafloor (Figs 2 and 3). The area on top of the slope is gener-

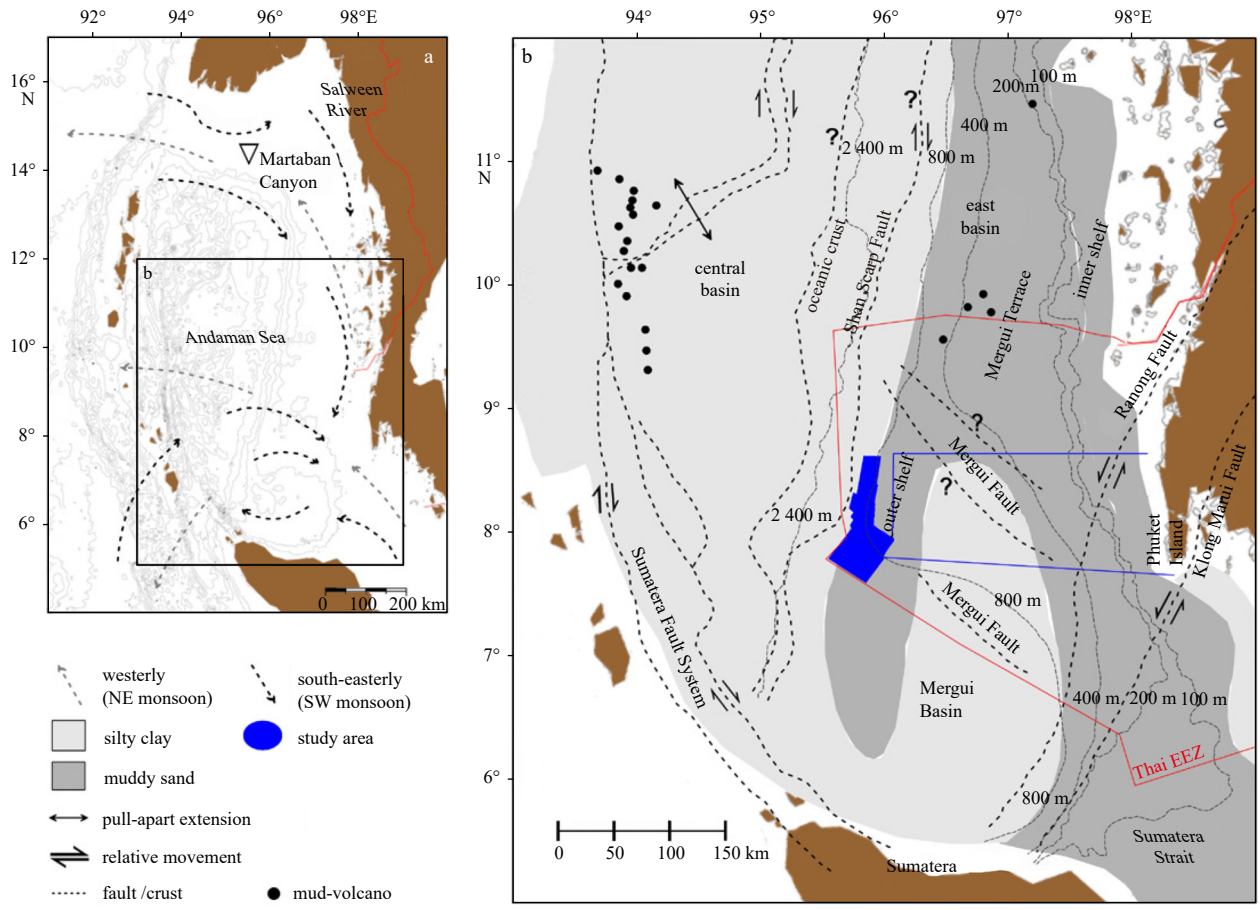

Fig. 1. Synthetic maps showing location of the Andaman Sea in the Northeast Indian Ocean. Patterns of seasonal sea-surface circulation including the westerly currents (NE monsoon) and the south-easterly currents (SW monsoon) are summarily redrawn from Rodolfo (1969) (a). The tectonic setting of the Andaman Basin redrawn from Curry (2005). Sediment textures covering the basin are redrawn from Rodolfo (1969). The blue box shows the investigated area (b). EEC: exclusive economic zone.

ally rather smooth and slightly inclined southward, while the area on the outer shelf break steepens westward with gradients varying from 1° to 4.8°, and is cut by gullies. Gradient on the N–S profile, including Profiles NS1-1 and NS1-2 at a water depth between 500 m and 600 m, shows an inclination angle of less than 0.08°. Several profiles between NS2-1 and NS2-4 reveal ruggedness and unevenness of slope morphology on the slope below the smooth area. Interestingly, Profiles NS3-1, NS3-2, and NS3-3 show that most of the areas on down slope at water depth below 1 200 m are strongly dissected by gullies (Figs 3a, b). In contrast, the different inclination angles on the E–W profiles allow dividing of the area on the slope into two subtle zones including the upper slope and the middle slope. The upper slope covers the area on the northern part of the shelf, where gradients range from 1.5° to 2.2° at water depth 600–900 m, and the southern end of the investigated area, where the gradient is approximately 1° at 700–1 200 m water depth. The middle slope occupies the area where gradients vary from 3° along the southern part at 900–1 300 m water depth to 4.8° further north (Figs 3a, c). In addition, there are few small indications of possible submarine landslides on the northern (Fig. 4a) and the middle part (Fig. 4b) of the slope. Plateaus or possible low oceanic guyots (Figs 5a, b), and several sizes of gullies (Fig. 6a) are inferred from the bathymetry.

4.1 *Submarine landslides*

The northernmost landslide is studied from the steep slope of the shelf break at a water depth of approximately 870 m. The sliding is located at 8°29′N and 95°53.65′E and oriented on an E–W direction perpendicular to the slope. The main scarp is not clearly identified from the bathymetry, however, it may lie below the escarpment. Shape of the slide scar seems to be an irregular and half ellipse-like with an estimated size of about 600 m width and 2.8 km length. Travel distance of the slide, which is estimated on Profile aa′, is approximately 1.2 km. The displaced mass is an irregular half ellipse-liked shape with an estimated size of 700 m width, 2 km length and 18 m height, resulting in a maximum approximated volume of 4×10^7 m^3 of displaced mass. Subbottom profiler records along Profile bb′ shows the echo-character of the failed mass (Fig. 4a). The echogram shows weak, transparent subbottom reflectors with varying vertex elevations above the seafloor and either little or no penetration (Damuth and Hayes, 1977; Damuth, 1980; Pratson and Laine, 1989). This could correspond to a rough-seafloor covered with sediments due to the deposition of mass wasting processes (Damuth, 1975; Domzig et al., 2009).

Another possible submarine landslide is studied from bathymetry at the middle part of a steep slope at water depth of about 945 m. The slide locates at 8°12.85′N and 95°48.75′E and is oriented on an E–W direction. The slide scar and failed mass are trapezoid-liked shapes. Size of the scar is estimated at 750 m width and 1.25 km length, and it incises as much as 25 m into the underlying sediments. The travel distance is approximately 700 m. The potential size of the mass failure is approximately

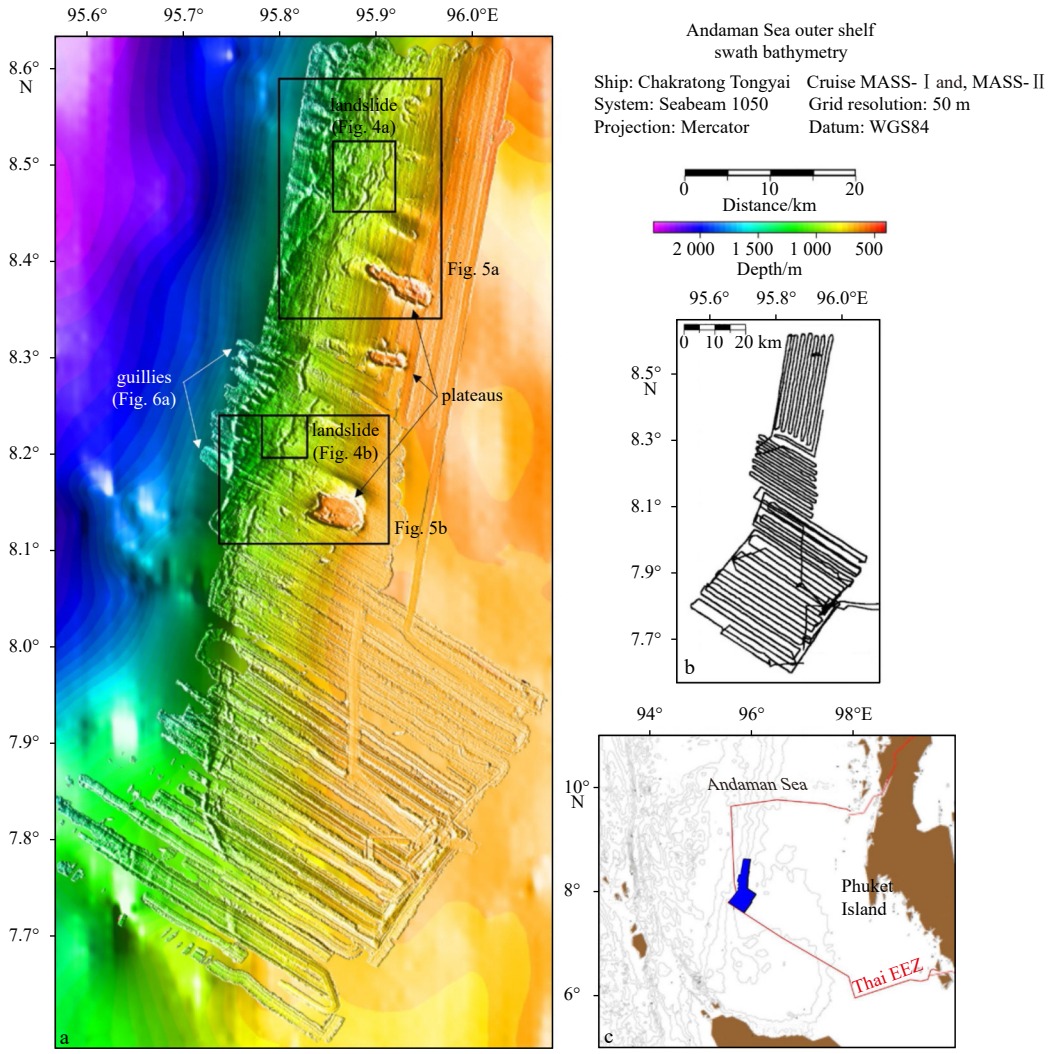

Fig. 2. A new detailed bathymetry of the upper slope of the Andaman Sea outer shelf is overlain on GEBCO 30-arc second GDA (The GEBCO_08 Grid, 2010) (a) and complements them with ship track-lines (b) and location of the study area (c). The investigated area is shown by a blue box. Detailed information in submarine landslides are shown in Figs 4a and b, plateaus are shown in Figs 5a and b, and gullies are shown in Fig. 6a.

1 100 m in width, 800 m in length and results in a maximum approximated volume of 2.2×10^7 m^3 of displaced mass. A subbottom Profile cc′ across the sliding indicates different phases of failure processes. The first slide is about 13 m in height, followed by a second slide of 10 m in height. At about 2.5 km of slide distance, the convex-upward slope profiles probably correspond to the sediment deposited from this failure (Fig. 4b). The echo-character of these deposits shows weak, transparent subbottom reflectors that could represent sediment mobility and deposits (Pratson and Laine, 1989).

4.2 *Large plateaus surrounded by moats*

The large conspicuous features which were exposed by the new detailed bathymetry are three plateau-like structures. These elliptical shaped plateaus generally locate on the middle part to the north of the upper slope between 8°07′N to 8°24′N and 95°50′E to 95°57′E (Fig. 2). Their size ranges from less than 10 to more than 20 km^2. The plateaus protrude to a height of about 50 m towards the shelf and height of about 200 m towards the slope. Their edges are bounded by rather steep vertical slopes. All plateaus show the presence of cracks around their edges and deep moats surrounding them. Although the plateaus have many features in common, there are distinct differences such as their volumes and sizes of the moats surrounding them. Sizes of the moats vary from a few hundred meters up to more than 4 km width (Fig. 5). Approximated by the bathymetry, the moats on the northern side are generally much deeper and wider than on the southern side. The moat of the southern plateau is much wider and more pronounced than the others (Fig. 5a). This plateau also shows the smoothest surface except for the southwestern quadrant that displays the presence of several sub-rounded depressions up to few hundred meters in diameter (Fig. 5b). The middle and northern plateaus show a rather smooth surface on their western half while the eastern half is more irregular. These two plateaus also show an irregular, hummocky surface at the western down-dip slope of the continuation of the plateaus that could represent slump deposits from disintegration of part of the plateaus. However, unequivocal interpretation of the observed features is not possible with the current data set.

Morphologically, the plateaus-like structures resemble guyots, i.e., drowned coral atolls. However, irregular surfaces on the eastern part of the middle and northern plateaus are not con-

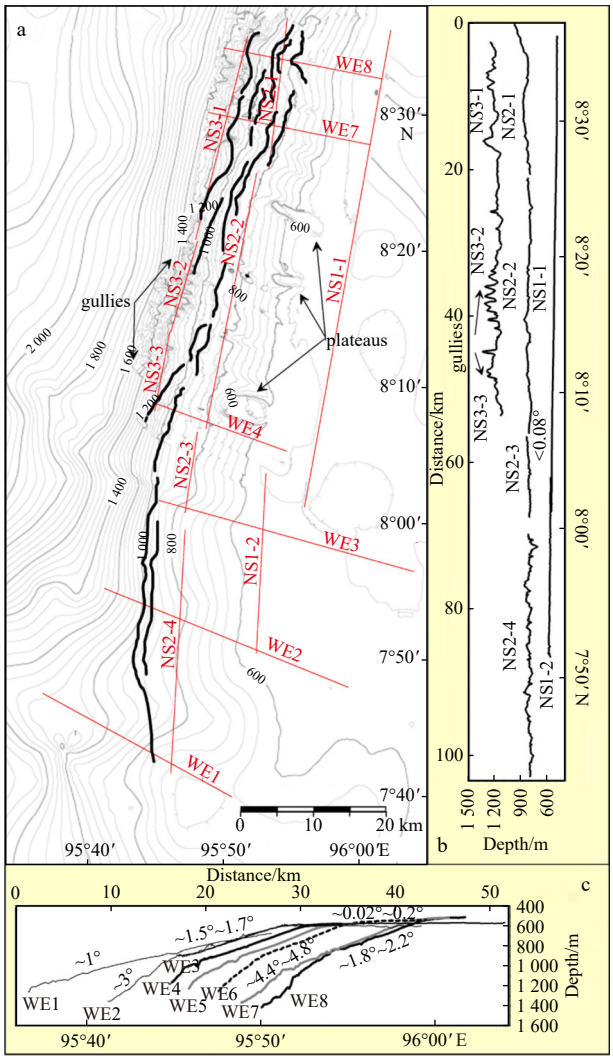

Fig. 3. Interpretation of the bathymetry shows prominent features, including three large plateaus surrounded by moats (a) . Drawn lines of slope ruggedness are shown by black lines. Contour interval is 40 m. Latitudinal (NS1-1 to NS3-3) (b) and longitudinal profiles (c)(WE1 to WE8) show the general morphological trends of the Andaman Sea outer shelf and upper slope.

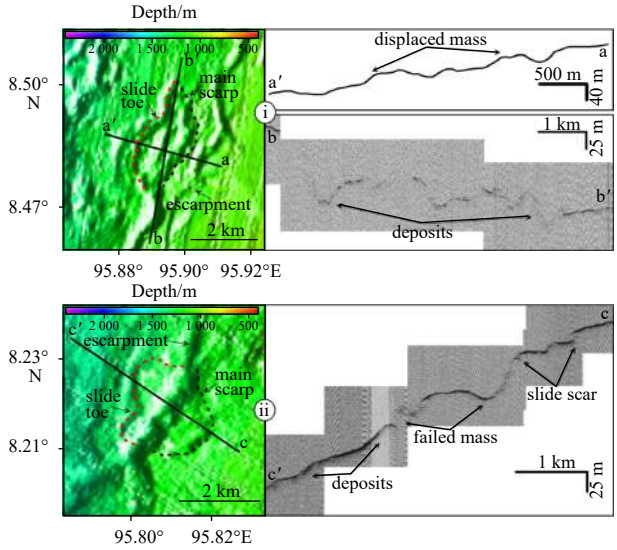

Fig. 4. Color-coded shaded relief maps with interpretation showing possible submarine landslides on the northernmost (i) and the middle part (ii) of the Andaman outer shelf and upper slope. Black dotted-lines show approximated slide scars, while red dotted-lines show approximated slide toes. Profile aa′ and a subbottom profiler record along Profile cc′ show a slide scar and convex-upward slopes that could represent displaced mass and slide deposits. Echo-character along Profile bb′ presents possible sediment deposit. For locations of both slides refer to Fig. 2.

sistent with this interpretation. Subbottom profiler records over the plateaus show prolonged echoes of about 10 m thickness with no subbottom reflectors (Fig. 5). This echo type could be interpreted as coarse-grained sediment cover on top of the plateau, similar to the echo-type defined by Damuth (1980) for 3.5 kHz echograms. Sediments covering the Mergui Ridge consist of sand and foraminiferal ooze, or sandstone and coral reef limestone (Rodolfo, 1969; Polachan and Racey, 1993; Saidova, 2008). Consequently, we interpret the plateaus as old coral structures or atolls that are blanketed by sediment deposits. The edges of the plateaus show numerous signs of disintegration of already consolidated deposits. Additional data are clearly required in order to clarify the nature and evolution of these structures.

Correlation between the bathymetry, backscattering imagery, and the high frequency subbottom profiles allowed the construction of a map showing possible main sedimentary deposit (Fig. 5) throughout the study area. Turbidity currents and/or mass transport deposit could dominate on large area on the area. We have no mean to distinguish sedimentary process because of incomplete swath bathymetric data and no sediment information from coring. However, the echo-type returning from the area and associated with a typical echo-type showing distinct, continuous, steeply dipping bottom echo with dipping subbottom reflectors indicate hemipelagic sedimentation and/or slump deposited by mass wasting (Damuth and Hayes, 1977; Damuth, 1980; Pratson and Laine, 1989). The finding suggests that the area could attribute to quiescent hemipelagic materials transport and deposit as slumps. Character of the echo reflections suggests a high degree of sediment mobilization and thus deposits may be from turbidity currents or debris flows. The high amplitude reflections perhaps testify to the presence of coarse sediments.

4.3 *Ruggedness and evenness of the outer shelf morphology*

On the northern part of survey area, the slope is characterized by various escarpments or slope failure lineaments. They represent active sediment movements or recent mass wasting processes. Several negative reliefs are also studied. They could be attributed to a pockmark or remobilized block that reaches 1 000 m in length 200 mm, in width and 30 mm in depth. In addition, one negative relief near the northern plateau corresponding to a scar is studied. Ripples below the scar indicating that sediment bypass may be reshaped by sediment flowing from the upper slope (Figs 3 and 4). On the backscatter imagery, there are two pieces of evidence suggestive of active sedimentary transits on the middle part of the area.

On the middle part of survey area, three plateaus are studied. They protrude high, more than 50 m above the smooth seafloor and, exceed the upper slope by more than 200 m. Their edges have sharp morphology with gradients of up to more than 50° and they are surrounded by moats (Figs 2 and 5). One elongated depression that could be attributed to a pockmarks is also observed near the middle plateau (Fig. 2). The size of the pockmark

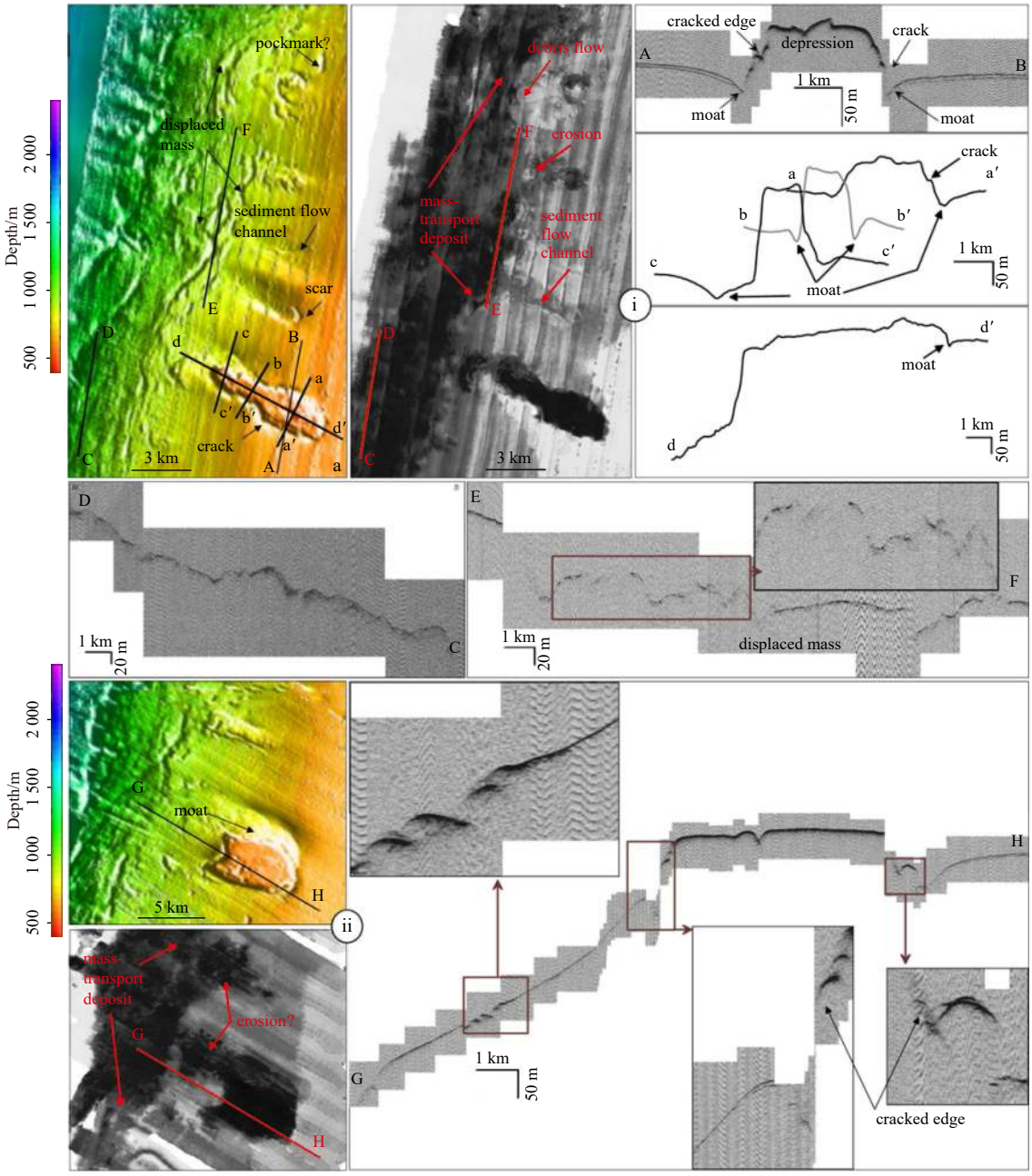

Fig. 5. Morphology of the northern plateau (i) and the southern plateau (ii) are shown by bathymetry, backscattering imagery and their high frequency subbottom profiles. The boundaries of possible sediment failure deposits are marked by red dotted lines. Locations of plateaus refer to Fig. 2.

is approximately 1 km in length and 30 m in depth. The foot of the middle slope is strongly dissected by many gullies or possibly heads of canyons (Fig. 6). The inter-canyon areas also have sharp morphology. Their walls have very steep slopes of up to more than 45°. On the backscatter imagery, there are various pieces of evidence of active sedimentary transits on the area, especially on the area below plateaus.

On the south, several escarpments or possible fault traces, generally lying on N–S direction, are observed on the slope. Their sizes vary from a few kilometers to more than 20 km with gradients of approximately 30°. Eleven possible locations of small slumps (Fig. 3a) are observed on subbottom profiler records. Their sizes vary between 500 m and 1 000 m in length and 10–20 m in height. Distributions of the slumps cover an area on approximate 200 km^2. The echo character is a distinct, continuous, steeply dipping bottom echo with dipping subbottom reflectors. The echo type generally represents quiescent hemipelagic sedimentation and/or slump deposited by mass wasting processes (Pratson and Laine, 1989). Due to no several continuous backscattering data being available near the southern part of the investigated area, the backscatter imagery does not allow discussion of the activity of possible fault traces and slope failures.

5 Discussion

Morphometric analysis of the sounding data acquired from the Andaman outer shelf and upper slope within the Thai EEZ reveals some indications of recent mass wasting that led to the possible slope failure events in a relatively steep slope in different

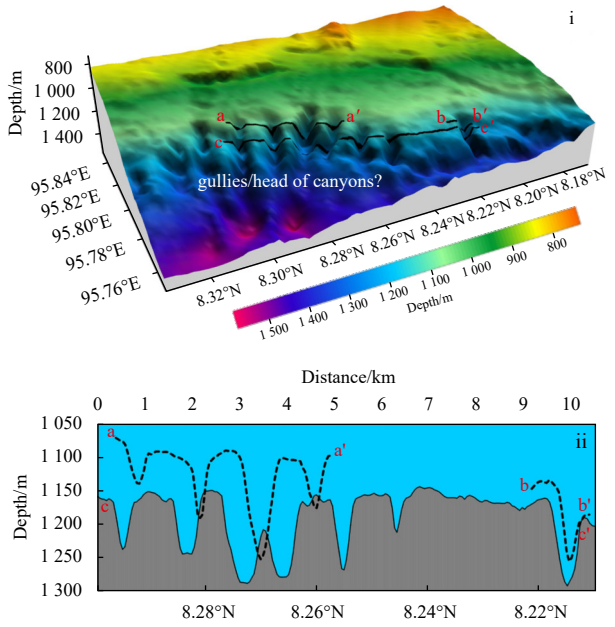

Fig. 6. A color-codes shaded 3D map showing gullies or possible head of canyons (i) and cross section along Profile aa′, bb′, and cc′ (ii). Locations of gullies refer to Fig. 2.

domains. The presence of many anomalous features on the seafloor are prerequisites for the generation of large submarine landslides (Hampton et al., 1996; Mulder and Cochonat, 1996). In addition, the sounding allows the characterization of a few previously unknown submarine landslides on the slope, which confirm the occurrence of slope failures. These features include large sediment transports from the Irrawaddy and the Salween rivers to the deep basin and eventually rapid deposition, and the occurrence of large earthquakes at close distance. It seems that events leading to slope failures have occurred in the different geological times.

Close analysis of a new detailed bathymetry and subbottom profiler record presented in this paper, shows two distinct submarine landslides. The first landslide is located at 8°29′N and 95°53.65′E in the northernmost part of the studied area (Fig. 4a). Another small landslide is situated in the middle part of the slope at position 8°12.85′N and 95°48.75′E (Fig. 4b). On the basis of the morphology of the failed mass, the difference between its depth (H) and the length (L) are likely key characteristic of the slides, and this suggests the need for classification of the submarine landslides using the Skempton ratio (Mulder and Cochonat, 1996). The ratio for first slide (the depth H = 77 m, and the length L = 1 600 m), which is estimated from bathymetric data, is H/L = 0.05. For the other slide, the ratio (the depth H = 85 m, and the length L = 2 238 m) estimated from subbottom profiler records is H/L = 0.04. These valuable estimations suggest that both slides correspond to translational submarine landslides (Mulder and Cochonat, 1996).

The theoretical tsunami wave length and maximum amplitude directly over the slope failure generated by disintegrative submarine landslides can be calculated by the semi empirical equations proposed by Watts et al. (2003) and McAdoo and Watts (2004). Following the equations, the calculations show that the northernmost landslide would have generated a tsunami wave of about 3 877 m wave length and with a maximum wave height of about 0.19 m, while the middle slide would have generated of about 4 454 m wave length and maximum approximately 0.14 m wave height. These initial wave characteristics could be input criteria for tsunami propagation models (Synolakis et al., 2002; Brune et al., 2010a, b, c) in order to calculate wave propagation and potential tsunami run-up onshore. However, the small initial wave height indicates that the observed submarine landslides are not the potential for generating a devastating coastal tsunami. It is consequently unlikely that submarine sliding has contributed to tsunami hazards along the Andaman Sea coast in the recent geological past. Only small landslides offshore of the Indonesian Sunda Arc have been found by Brune et al. (2010b). The reason for the absence of large tsunami-generating landslides might be found in the nature of the sediments at the Andaman Sea outer shelf and upper slope. Both subbottom profiler records (Fig. 4) and published data on sediment textures and sedimentation rate from Rodolfo (1969), Polachan and Racey (1993), and Saidova (2008), suggest the presence of sandy deposits that would be well drained, precluding the build-up of overpressure.

The surveyed area on southwestern part of slope of the Mergui Ridge is generally rather smooth, while the west rim of the middle and the north part is steepens with gradients up to 4.8° to the north and is cut by gullies. Regarding sediment types and sedimentation rates, sediments mainly consist of foraminiferal oozes on top of the ridge, while silty clays prevail in the adjacent area. Rodolfo (1969) described relict foraminifera and relict corals in modern sediments of the Mergui area, implying that sedimentation rates on the Mergui Ridge are generally low and/or mainly related to biogenic input. This sequence described to exhibit mass flow deposits might be particularly effective potential tsunami generations without large displacements. However, more information from seismic and bathymetric data for calculation the volume of mass-wasting events is an important factor for their tsunami potential to quantify individual mass-wasting events and tsunamis wave propagation model in the near future.

6 Conclusions

Slope instabilities are revealed along the study area. It is surprising that this slope is rather poorly sediment accumulated. However, this confirms the importance of structural control in the shaping and evolution of submarine domains. The various segments of the slope exhibit contracting slope instabilities.

The areas on the northern and the middle parts of the slope are strongly affected by mass wasting processes such as erosion, debris flow and slumping. These events seem recurrent and define blocks. The driving mechanism seems to be the tilting of the slope and consequent gravity instabilities. The tilting allows the sediment on the upper part to slide downslope. Various pieces of evidence and parallel lineaments of slope failures suggest that the sliding occurred at difference times, but is recently occurring. On the southern part of the study area, eleven slum locations are studied based on subbottom profiler records.

Two locations indicated possible submarine landslides are studied on the slope, maximum approximated volumes of both displaced masses are 4.8×10^7 m^3 and 2.2×10^7 m^3.

There is no evidence that the sliding has generated tsunamis, but slides exhibit occurring slope failures and mass movements, leading to slope instability assessment.

Acknowledgements

We acknowledge the Leibniz Institute of Marine Science (IFM-GEOMAR) and Southeast Asia START Regional Center for facilitating cooperative research between Thai and German scientists. We acknowledge the help of: Wilhelm Weinrebe, Ingo Klaucke, Sebastian Krastel, Ernst Flueh, Warner Brueckmann,

Christian Hensen, and Suratta Bunsomboonsakul. We are grateful to Captain. Chonwat Singnu and his crew who made the cruises successful. The authors would like to especially thank Katja Lindhorst who gave a nice introduction to software KINGDOM Suite, Colin Tosh for English proofreading and Chantima Piyapong for editing the revised manuscript.

References

Bellec V K, Bøe R, Rise L, et al. 2010. Rippled scour depressions on continental shelf bank slopes off Nordland and Troms, Northern Norway. Continental Shelf Research, 30(9): 1056–1069, doi: 10.1016/j.csr.2010.02.006

Beyer A, Rathlau R, Schenke H W. 2005. Multibeam bathymetry of the Håkon Mosby mud volcano. Marine Geophysical Researches, 26(1): 61–75, doi: 10.1007/s11001-005-1131-8

Beyer A, Schenke H W, Klenke M, et al. 2003. High resolution bathymetry of the eastern slope of the Porcupine Seabight. Marine Geology, 198(1–2): 27–54, doi: 10.1016/S0025-3227(03)00093-8

Brune S, Babeyko A Y, Gaedicke C, et al. 2010a. Hazard assessment of underwater landslide-generated tsunamis: a case study in the Padang region, Indonesia. Natural Hazards, 53(2): 205–218, doi: 10.1007/s11069-009-9424-x

Brune S, Babeyko A Y, Ladage S, et al. 2010b. Landslide tsunami hazard in the Indonesian Sunda Arc. Natural Hazards and Earth System Sciences, 10(3): 589–604, doi: 10.5194/nhess-10-589-2010

Brune S, Ladage S, Babeyko A Y, et al. 2010c. Submarine landslides at the eastern Sunda margin: observations and tsunami impact assessment. Natural Hazards, 54(2): 547–562, doi: 10.1007/s11069-009-9487-8

Bull S, Cartwright J, Huuse M. 2009. A review of kinematic indicators from mass-transport complexes using 3D seismic data. Marine and Petroleum Geology, 26(7): 1132–1151, doi: 10.1016/j.marpetgeo.2008.09.011

Caress D W, Chayes D N. 2004. MB-System Version 5, Open source software distributed.http://www.mbari.org/data/mbsystem/ [2003-12-05]

Curray J R. 2005. Tectonics and history of the Andaman Sea region. Journal of Asian Earth Sciences, 25(1): 187–232, doi: 10.1016/j.jseaes.2004.09.001

Chough S K, Lee S H, Kim J W, et al. 1997. Chirp (2–7 kHz) echo characters in the Ulleung Basin. Geosciences Journal, 1(3): 143–153, doi: 10.1007/BF02910206

Damuth J E. 1975. Echo character of the western equatorial Atlantic floor and its relationship to the dispersal and distribution of terrigenous sediments. Marine Geology, 18(2): 17–45, doi: 10.1016/0025-3227(75)90047-X

Damuth J E. 1978. Echo character of the Norwegian-Greenland Sea: relationship to Quaternary sedimentation. Marine Geology, 28(1–2): 1–36, doi: 10.1016/0025-3227(78)90094-4

Damuth J E. 1980. Use of high-frequency (3.5–12 kHz) echograms in the study of near-bottom sedimentation processes in the deep-sea: a review. Marine Geology, 38(1–3): 51–75, doi: 10.1016/0025-3227(80)90051-1

Damuth J E, Hayes D E. 1977. Echo character of the East Brazilian continental margin and its relationship to sedimentary processes. Marine Geology, 24(2): 73–95, doi: 10.1016/0025-3227(77)90002-0

de Alteriis G, Passaro S, Tonielli R. 2003. New, high resolution swath bathymetry of Gettysburg and Ormonde Seamounts (Gorringe Bank, eastern Atlantic) and first geological results. Marine Geophysical Researches, 24(3): 223–244, doi: 10.1007/s11001-004-5884-2

Domzig A, Gaullier V, Giresse P, et al. 2009. Deposition processes from echo-character mapping along the western Algerian margin (Oran-Tenes), Western Mediterranean. Marine and Petroleum Geology, 26(5): 673–694, doi: 10.1016/j.marpetgeo.2008.05.006

Hampton M A, Lee H J, Locat J. 1996. Submarine landslides. Reviews of Geophysics, 34(1): 33–59, doi: 10.1029/95RG03287

IOC, IHO, and BODC, 2003 , "Centenary Edition of the GEBCO Digital Atlas", published on CD-ROM on behalf of the Intergovernmental Oceanographic Commission and the International Hydrographic Organization as part of the General Bathymetric Chart of the Oceans; British Oceanographic Data Centre, Liverpool.

Jackson P D, Gunn D A, Long D. 2004. Predicting variability in the stability of slope sediments due to earthquake ground motion in the AFEN area of the western UK continental shelf. Marine Geology, 213(1–4): 363–378, doi: 10.1016/j.margeo.2004.10.014

Jenkins C J, Keene J B. 1992. Submarine slope failures of the southeast Australian continental slope: a thinly sedimented margin. Deep-Sea Research Part A: Oceanographic Research Papers, 39(2): 121–136, doi: 10.1016/0198-0149(92)90100-8

Khan P K, Chakraborty P P. 2005. Two-phase opening of Andaman Sea: a new seismotectonic insight. Earth and Planetary Science Letters, 229(3–4): 259–271, doi: 10.1016/j.epsl.2004.11.010

Lee H, Baraza J. 1999. Geotechnical characteristics and slope stability in the Gulf of Cadiz. Marine Geology, 155(1–2): 173–190, doi: 10.1016/S0025-3227(98)00146-7

Lee H J, Syvitski J P M, Parker G, et al. 2002. Distinguishing sediment waves from slope failure deposits: field examples, including the 'Humboldt slide', and modelling results. Marine Geology, 192(1–3): 79–104, doi: 10.1016/S0025-3227(02)00550-9

Levchenko O V, Verzhbitskii V E, Lobkovskii L I. 2008. Submarine landslide structures in neopleistocene deposits on the western slope of the Derbent basin of the Caspian Sea. Oceanology, 48(6): 864–871, doi: 10.1134/S000143700806012X

Leynaud D, Mienert J, Vanneste M. 2009. Submarine mass movements on glaciated and non-glaciated European continental margins: a review of triggering mechanisms and preconditions to failure. Marine and Petroleum Geology, 26(5): 618–632, doi: 10.1016/j.marpetgeo.2008.02.008

Locat J, Lee H, ten Brink U S, et al. 2009. Geomorphology, stability and mobility of the Currituck slide. Marine Geology, 264(1–2): 28–40, doi: 10.1016/j.margeo.2008.12.005

Loncke L, Droz L, Gaullier V, et al. 2009a. Slope instabilities from echo-character mapping along the French Guiana transform margin and Demerara abyssal plain. Marine and Petroleum Geology, 26(5): 711–723, doi: 10.1016/j.marpetgeo.2008.02.010

Loncke L, Gaullier V, Droz L, et al. 2009b. Multi-scale slope instabilities along the Nile deep-sea fan, Egyptian margin: a general overview. Marine and Petroleum Geology, 26(5): 633–646, doi: 10.1016/j.marpetgeo.2008.03.010

Masson D G, Watts A B, Gee M J R, et al. 2002. Slope failures on the flanks of the western Canary Islands. Earth-Science Reviews, 57(1–2): 1–35, doi: 10.1016/S0012-8252(01)00069-1

McAdoo B G, Watts P. 2004. Tsunami hazard from submarine landslides on the Oregon continental slope. Marine Geology, 203(3–4): 235–245, doi: 10.1016/S0025-3227(03)00307-4

Moscardelli L, Wood L, Mann P. 2006. Mass-transport complexes and associated processes in the offshore area of Trinidad and Venezuela. AAPG Bulletin, 90(7): 1059–1088, doi: 10.1306/02210605052

Mosher D C, Austin Jr J A, Fisher D, et al. 2008. Deformation of the northern Sumatra accretionary prism from high-resolution seismic reflection profiles and ROV observations. Marine Geology, 252(3–4): 89–99, doi: 10.1016/j.margeo.2008.03.014

Mulder T, Cochonat P. 1996. Classification of offshore mass movements. Journal of Sedimentary Research, 66(1): 43–57, doi: 10.1306/D42682AC-2B26-11D7-8648000102C1865D

Pan Xiaoyi, Li Linlin, Nguyễn P H, et al. 2022. Submarine landslides in the west continental slope of the South China Sea and their tsunamigenic potential. Frontiers in Earth Science, 10: 843173, doi: 10.3389/feart.2022.843173

Polachan S, Racey A. 1993. Lower Miocene larger foraminifera and petroleum potential of the Tai Formation, Mergui Group, Andaman Sea. Journal of Southeast Asian Earth Sciences, 8(1–4): 487–496, doi: 10.1016/0743-9547(93)90047-S

Pratson L F, Laine E P. 1989. The relative importance of gravity-induced versus current-controlled sedimentation during the

Quaternary along the Mideast U. S. outer continental margin revealed by 3.5 kHz echo character. Marine Geology, 89(1–2): 87–126, doi: 10.1016/0025-3227(89)90029-7

Raju K A K, Ramprasad T, Rao P S, et al. 2004. New insights into the tectonic evolution of the Andaman Basin, Northeast Indian Ocean. Earth and Planetary Science Letters, 221(1–4): 145–162, doi: 10.1016/S0012-821X(04)00075-5

Ramaswamy V, Rao P S, Rao K H, et al. 2004. Tidal influence on suspended sediment distribution and dispersal in the northern Andaman Sea and Gulf of Martaban. Marine Geology, 208(1): 33–42, doi: 10.1016/j.margeo.2004.04.019

Rao P S, Ramaswamy V, Thwin S. 2005. Sediment texture, distribution and transport on the Ayeyarwady continental shelf, Andaman Sea. Marine Geology, 216(4): 239–247, doi: 10.1016/j.margeo.2005.02.016

Reddy D R, Rao T S. 1997. Echo characters of the continental margin, western Bay of Bengal, India. Marine Geology, 140(1–2): 201–217, doi: 10.1016/S0025-3227(97)00016-9

Rodolfo K S. 1969. Sediments of the Andaman Basin, northeastern Indian Ocean. Marine Geology, 7(5): 371–402, doi: 10.1016/0025-3227(69)90014-0

Saidova K M. 2008. Benthic foraminifera communities of the Andaman Sea (Indian Ocean). Oceanology, 48(4): 517–523, doi: 10.1134/S0001437008040073

Seeber L, Mueller C, Fujiwara T, et al. 2007. Accretion, mass wasting, and partitioned strain over the 26 Dec 2004 Mw 9.2 rupture offshore Aceh, northern Sumatra. Earth and Planetary Science Letters, 263(1–2): 16–31, doi: 10.1016/j.epsl.2007.07.057

Silva A J, Baxter C D P, LaRosa P T, et al. 2004. Investigation of mass wasting on the continental slope and rise. Marine Geology, 203(3–4): 355–366, doi: 10.1016/S0025-3227(03)00315-3

Sultan N, Cochonat P, Canals M, et al. 2004. Triggering mechanisms of slope instability processes and sediment failures on continental margins: a geotechnical approach. Marine Geology, 213(1–4): 291–321, doi: 10.1016/j.margeo.2004.10.011

Sultan N, Voisset M, Marsset B, et al. 2007. Potential role of compressional structures in generating submarine slope failures in the Niger Delta. Marine Geology, 237(3–4): 169–190, doi: 10.1016/j.margeo.2006.11.002

Sun Qiliang, Cartwright J, Xie Xinong, et al. 2018. Reconstruction of repeated Quaternary slope failures in the northern South China Sea. Marine Geology, 401: 17–35, doi: 10.1016/j.margeo.2018.04.009

Sun Qiliang, Leslie S. 2020. Tsunamigenic potential of an incipient submarine slope failure in the northern South China Sea. Marine and Petroleum Geology, 112: 104111, doi: 10.1016/j.marpetgeo.2019.104111

Synolakis C E, Bardet J P, Borrero J C, et al. 2002. The slump origin of the 1998 Papua New Guinea Tsunami. Proceedings of the Royal Society A: Mathematical, Physical and Engineering Sciences, 458(2020): 763–789, doi: 10.1098/rspa.2001.0915

Terry J P, Winspear N, Goff J, et al. 2017. Past and potential tsunami sources in the South China Sea: a brief synthesis. Earth-Science Reviews, 167: 47–61, doi: 10.1016/j.earscirev.2017.02.007

The GEBCO_08 Grid. 2010. version 20100927. http://www.gebco.net [2010-10-25]

Tingay M R P, Morley C K, Hillis R R, et al. 2010. Present-day stress orientation in Thailand's basins. Journal of Structural Geology, 32(2): 235–248, doi: 10.1016/j.jsg.2009.11.008

Vanneste M, Mienert J, Bünz S. 2006. The Hinlopen Slide: a giant, submarine slope failure on the northern Svalbard margin, Arctic Ocean. Earth and Planetary Science Letters, 245(1–2): 373–388, doi: 10.1016/j.epsl.2006.02.045

von Huene R, Ranero C R, Watts P. 2004. Tsunamigenic slope failure along the Middle America Trench in two tectonic settings. Marine Geology, 203(3–4): 303–317, doi: 10.1016/S0025-3227(03)00312-8

Watts P, Grilli S T, Kirby J T, et al. 2003. Landslide tsunami case studies using a Boussinesq model and a fully nonlinear tsunami generation model. Natural Hazards and Earth System Sciences, 3(5): 391–402, doi: 10.5194/nhess-3-391-2003

Wessel P, Smith W H F. 1998. New, improved version of generic mapping tools released. Eos, Transactions American Geophysical Union, 79(47): 579, doi: 10.1029/98EO00426